ELSEVIER

Journal of Organometallic Chemistry 657 (2002) 75–82

Journal of Organo metallic Chemistry

www.elsevier.com/locate/jorganchem

High resolution solid state NMR investigation of various boron nitride preceramic polymers

Christel Gervais, Florence Babonneau *

Chimie de la Matière Condensée, Université Pierre et Marie Curie, 4 Place Jussieu, 75005 Paris, France

Received 3 September 2001; accepted 14 May 2002

Abstract

Hexagonal boron nitride (h-BN) ceramics can be prepared from polymeric precursors by heat treatment under inert atmosphere. The purpose of this paper is to illustrate the strategy that can be followed to characterize by ^{15}N and ^{11}B solid state NMR the polymers as well as their pyrolysis derivatives. A suitable choice of NMR techniques, combined with isotopic enrichment, can lead to a good qualitative as well as quantitative description of the local environment of B and N sites in such complex samples. © 2002 Elsevier Science B.V. All rights reserved.

Keywords: Solid state NMR; Boron nitride; Polyborazilene; Poly(aminoborane)

1. Introduction

Polymeric route to refractory nonoxide ceramics is a process of great interest offering possibilities of obtaining composite and shaped materials such as fibres, films or bulk pieces from soluble or fusible starting polymers [1]. It has been first developed to produce SiC or SiCN-based ceramics, starting from polysilanes, polycarbosilanes and polysilazanes [2,3]. More recently, this approach was extended to the preparation of hexagonal boron nitride (h-BN), a ceramic widely used in high temperature technology [4]. Different families of polymeric precursors have been developed by several groups, starting from borazine ($B_3N_3H_6$), or N- and B-substituted borazines [4–10]. Also, polyborosilazanes have been synthesized by different synthetic routes [11–17]; the resulting Si–B–C–N ceramics exhibit exceptional high-temperature stability [18], and high oxidation resistance [13].

In this chemical route to ceramics, the polymer architecture may strongly influence the structure of the final ceramic. It is therefore essential to rely on characterization tools to get a precise description of the polymer structure, and then to be able to follow step-by-step the polymer-to-ceramic conversion, that will generate through complex reactions, intermediates with distribution of sites. The samples usually do not present any long range order, which prevents the use of X-ray diffraction. Indeed, in this field, high resolution solid state magic angle spinning nuclear magnetic resonance (MAS NMR) has been shown to be extremely useful, especially for Si–C polymer-derived ceramics due to the relatively good NMR responses of ^{29}Si and ^{13}C nuclei [19]. For BN-containing ceramics, the NMR characterisation was more challenging, because of a terrible lack of sensitivity of the ^{15}N isotope in natural abundance (3.8×10^{-6} compared with ^{1}H) and a lack of resolution of the ^{11}B solid state NMR spectra due the quadrupolar character of this isotope.

However, by an appropriate combination of solid state NMR techniques, which helps in improving resolution and spectral edition (double resonance experiments ($\{^{1}H\}-\{X\}$, $X = {}^{15}N$ or ^{11}B), multi-quantum (MQ) MAS sequence for quadrupolar nuclei, use of high magnetic fields), a good description of the various N and B sites (coordination number as well as nature of the first and even second neighboring atoms) can be obtained. The use of these techniques will be illustrated

---

* Corresponding author. Present address. Laboratoire de Chimie de la Matière Condensée, Université Pierre et Marie Curie, 4 Place Jussieu, Tour 54, Etage 5, 75252 Paris Cedex 05, France. Tel.: +33-1-44274135; fax: +33-1-44274769

E-mail address: fb@ccr.jussieu.fr (F. Babonneau).

PII: S0022-328X(02)01586-3

in the following sections for various boron nitride preceramic polymers, and their pyrolysis derivatives.

2. Experimental

2.1. Sample preparation

Three preceramic polymers have been studied. The polyborazilene, called Pol(Δ) was prepared by a procedure proposed in the literature [5] that consists in thermal dehydropolymerization of borazine. A quick one-step procedure to obtain borazine from sodium borohydride and ammonium sulfate was recently proposed [20]. The polyborazilene, called Pol(NH_3) was synthesized by reacting borazine with NH_3 according to a procedure developed by Vaultier et al. [21]. As for the poly-(aminoborane) called PAB, it was prepared by a modified version of a procedure developed by Sneddon and Wideman [20], and described in a paper published by Kim et al. [22]. The ^{15}N enriched polymers were obtained from enriched borazine synthesized with ammonium sulfate ^{15}N enriched at 10 at.% purchased from Isotec.

2.2. NMR experiments

Solid state ^{15}N CP-MAS experiments were performed at room temperature (r.t.) on a Bruker MSL-300 spectrometer, at a frequency of 30.41 (^{15}N) and 300.13 MHz (^{1}H), using a Bruker CP-MAS probe. Solid samples were spun at 5 kHz, using 7 mm ZrO_2 rotors filled up in a glove-box under dried Ar atmosphere. All ^{15}N CP-MAS experiments were performed under the same Hartmann–Hahn match condition, set up by using a powdered sample of NH_4NO_3: both RF channel levels $\omega_{1H}/2\pi$ and $\omega_{15N}/2\pi$ were carefully set so that $|\omega_{1H}|/2\pi = |\omega_{15N}|/2\pi = 42$ kHz. Proton decoupling was always applied during acquisition and a repetition time of 10 s was used. The ^{15}N MAS NMR spectra were recorded with a pulse angle of 90° and a recycle delay between pulses of 60 s. Chemical shifts were referenced to solid NH_4NO_3 (10% ^{15}N enriched sample, δ_{iso} ($^{15}NO_3$) = −4.6 ppm compared to CH_3NO_2 ($\delta = 0$ ppm)).

^{11}B MAS NMR experiments were performed at r.t. on Bruker MSL-300 and MSL-400 spectrometers, at a frequency of 96.216 and 128.28 MHz, respectively, using a Doty CP-MAS probe with no probe background. Solid samples were spun at 10 kHz, using 5 mm ZrO_2 rotors filled up in a glove-box under dried argon atmosphere. A 1 μs single-pulse excitation (while the $t_{90°}$ measured on BF_3OEt_2 is 8 μs) was employed, with repetition times of 5 s. ^{11}B MAS experiments were also performed at 11.7 T on a Bruker ASX500 spectrometer and at 18.8 T on a Bruker DSX800 spectrometer using 4 mm ZrO_2 rotors. The ^{11}B MQ-MAS and ^{11}B CP/MAS experiments has been acquired using a Bruker DSX400 equipped with a 4 mm Bruker CP-MAS probehead, at a spinning rate of 10 kHz. Details on the parameters used for these experiments have been given in a previous publication [23]. All ^{11}B chemical shifts were determined relative to liquid BF_3OEt_2 ($\delta = 0$ ppm). The FIDs were analysed with the WIN-NMR Bruker program and simulations of the spectra were done with the WIN-FIT program [24].

3. Results and discussion

3.1. Preceramic polymers

Three boron nitride preceramic polymers have been studied: two polyborazilenes prepared from borazine, either through thermolysis (Pol(Δ)) or amonolysis (Pol(NH_3)) and a poly(aminoborane) $[NH_2BH_2]_n$ (PAB). The proposed structures for Pol(Δ) and PAB are schematically represented in Fig. 1. The structure of Pol(NH_3) is certainly more complex, as illustrated later in this paper.

The ^{15}N MAS NMR spectra of the three polymers are presented in Fig. 2. Due to the very low sensitivity of this isotope, the spectra of the nonenriched samples can only be recorded using ^{1}H cross-polarization, and with a rather long acquisition time. With 10 at.% enriched samples, both single pulse (SP) and cross-polarization (CP) experiments can be performed. The CP sequence is based on a polarization transfer between the abundant nuclei (^{1}H) and the rare nuclei (^{15}N), driven by the ^{1}H–^{15}N heteronuclear dipolar coupling, and is thus sensitive to the inter-nuclei distance. The comparison between the spectra clearly shows the large enhancement in sensitivity of the CP spectra, but also the loss of quantitativity, since the intensity of the CP signals depends on the proton environment of the various sites.

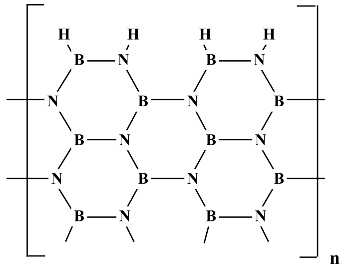
(a) – Pol(Δ)

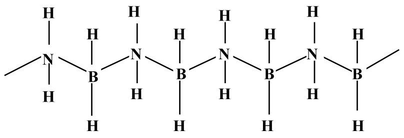
(b) – Pab

Fig. 1. Proposed structural models for Pol(Δ) and PAB.

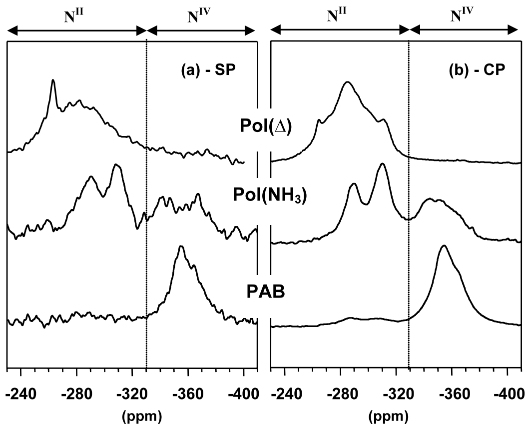

Fig. 2. ^{15}N MAS NMR spectra of the three ^{15}N-enriched polymers: (a) recorded with SP; (b) recorded with ^{1}H CP (contact time: 5 ms).

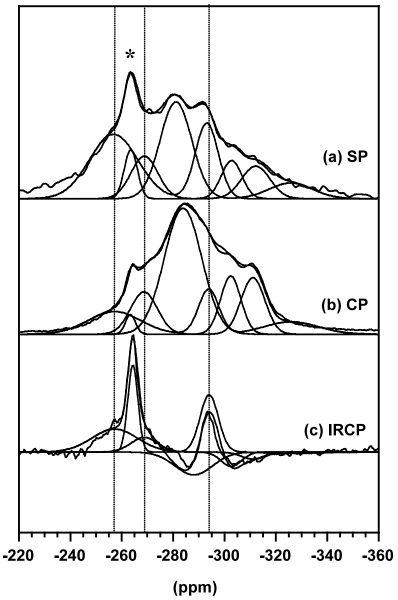

Fig. 3. ^{15}N MAS NMR spectra of Pol(Δ). (a) SP spectrum; (b) CP spectrum (contact time: 5 ms); and (c) IRCP spectrum (contact time: 5 ms; inversion time: 175 μs). (*): peak from residual borazine.

Two domains in chemical shift can be distinguished: from −250 to −330 ppm for tricoordinated N atoms (N^{III}) and from −330 to −400 ppm for tetracoordinated N atoms (N^{IV}) [25]. This figure clearly shows that one can identify easily the coordination number of the N sites in the various polymers: Pol(Δ) consists only of N^{III} sites as expected from the proposed model (Fig. 1), while the other two polymers present a mixture of both sites, mainly N^{IV} sites in PAB with traces of N^{III} also in agreement with the proposed structure (Fig. 1), while Pol(NH_3) is characterized by a large distribution of N^{III} and N^{IV} sites. However, the range of chemical shifts observed for Pol(Δ) and PAB suggests that the structural models presented in Fig. 1 are far too simplified, since only one $\mathit{N}H_2B$ site is expected in PAB and two $\mathit{N}HB_2$ and $\mathit{N}B_3$ sites in Pol(Δ).

In order to identify the various N sites with the same coordination number, one can use the inversion recovery cross polarization (IRCP) technique [26,27]. The only modification compared to the classical CP sequence is the introduction of a phase inversion after the contact time, that will induce a progressive inversion of the magnetization during an inversion time, t_i. The dynamics of inversion strongly depends on the $^{15}N–^{1}H$ dipolar coupling and the main advantage of this sequence compared to the standard CP sequence is that the magnetization starts from an optimum value, then decreases and becomes negative when increasing t_i. It is thus easy to visualize differences in inversion dynamics of various signals especially when they overlap. This sequence has already been successfully used to identify $^{15}NH_x$ sites ($x = 0–3$) [28]. Example of IRCP spectrum recorded on Pol(Δ) which contains only N^{III} sites, but with at least two types of environments, $\mathit{N}HB_2$ and $\mathit{N}B_3$ sites, is given in Fig. 3. It clearly shows that besides the sharp peak at −263 ppm due to residual borazine trapped in the polymer (*), the N sites can be indeed decomposed in two families. The signals due to $\mathit{N}HB_2$ sites, which are characterized by a strong $^{1}H–^{15}N$ dipolar coupling, invert faster than the signals due to $\mathit{N}B_3$ sites that correspond to weaker coupling. A detailed analysis of these spectra can be performed and lead to a quantification of the various sites, through the simulation of the SP spectrum (Fig. 3a) [23]. The multiplicity of sites suggests that the ^{15}N chemical shift value is sensitive not only to the nature of the first neighboring atoms (B or H) but also to the second ones (N or H). Indeed ab-initio calculations of chemical shifts have been performed on model clusters by Gastreich and Marian [29]. The clusters were built from edge-sharing B_3N_3 rings, and six types of tricoordinated N sites with different first and/or second neighboring atoms were identified, which are depicted in Fig. 4. The chemical shift values range from −253 to −305 ppm, in good agreement with our experimental data

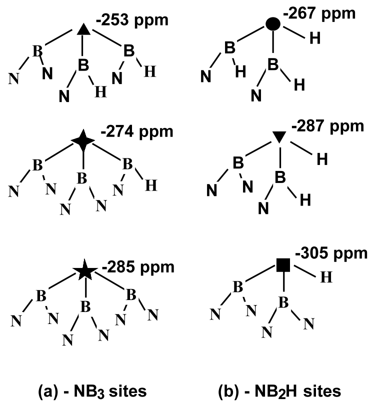

(a) - NB_3 sites (b) - NB_2H sites

Fig. 4. Nitrogen environments found in model clusters, used for ab initio calculations of ^{15}N chemical shift values [29].

(Fig. 3). The assignments of the various peaks will be discussed later with the results on the pyrolyzed samples.

The ^{11}B MAS NMR spectra of the three polymers are presented in Fig. 5. Two chemical shift ranges can be identified corresponding to tricoordinated B^{III} atoms (from 0 to 40 ppm), and to tetracoordinated B^{IV} atoms, (from −40 to 0 ppm). ^{11}B (80.22% naturally abundant) is a half-integer nucleus ($I = 3/2$) that possesses a quadrupolar momentum. This gives rise to a quadrupolar interaction whose amplitude will strongly depend on the distortion of the site compared to the cubic symmetry. When this interaction is strong, the second order terms of the interaction are only partially averaged by MAS, and this gives rise to a characteristic lineshape that can be seen in Fig. 5 for the B^{III} sites. For B^{IV} sites, the higher symmetry corresponds to a small quadrupolar coupling constant and the signals are nearly gaussian. This figure shows clearly that one can identify easily the coordination number of B sites. The results are similar to those found for the N sites: only B^{III} sites in Pol(Δ), a mixture of B^{III} and B^{IV} sites for Pol(NH_3) and mainly B^{IV} sites for PAB, with some B^{III} sites.

The broadness of the ^{15}N-NMR signals is essentially due to a distribution of chemical shift values, and an appropriate use of $\{^1H\}-^{15}N$ cross-polarization derived sequences allowed us to discriminate the various sites according to their proton environments. For ^{11}B-NMR signals, the linewidth mainly depends on the quadrupolar interaction. One-way to decrease it is to record spectra at higher magnetic fields as illustrated in Fig. 6, for Pol(Δ). At 18.8 T, the quadrupolar broadening of the B^{III} sites is considerably reduced, and one can distinguish two sites in Pol(Δ) assigned to BN_3 ($\delta_{iso} = 27$ ppm) and BHN_2 ($\delta_{iso} = 31$ ppm), in agreement with the proposed structural model (Fig. 1). In Pol(NH_3), the spectrum recorded at 18.8 T reveals the additional presence of tetracoordinated sites, BH_3N ($\delta_{iso} = -22$ ppm) and BH_2N_2 ($\delta_{iso} = -6$ and -12 ppm). Another way to get resolved spectra is to use two-dimensional (2D) ^{11}B multi-quantum (MQ) MAS sequence [30], from which an isotropic spectrum can be obtained. Such experiment was ran with Pol(Δ) under efficient proton decoupling: two signals are clearly seen in the isotropic dimension (Fig. 7). Combination of these data with the 1D MAS NMR spectra leads to the determination of the NMR parameters for each site (BN_3: $\delta_{iso} = 27$ ppm; $C_Q = 2.7$ MHz; $\eta = 0.1$; BHN_2: $\delta_{iso} = 31$ ppm; $C_Q = 2.9$ MHz; $\eta = 0.1$), and their quantification (BN_3–BHN_2 = 70:30). In contrast with the ^{15}N-NMR data, the ^{11}B chemical shift differences between the protonated (BHN_2) and nonprotonated sites (BN_3) is two small to allow sites with different second neighboring atoms to be distinguished.

A summary of the N and B sites which have been identified for the three polymers are listed in Table 1,

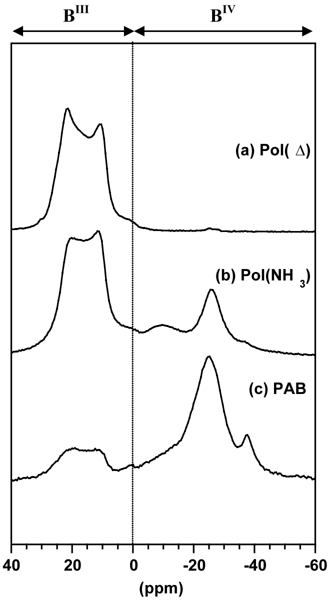

Fig. 5. ^{11}B MAS NMR spectra of the three polymers recorded at 9.4 T.

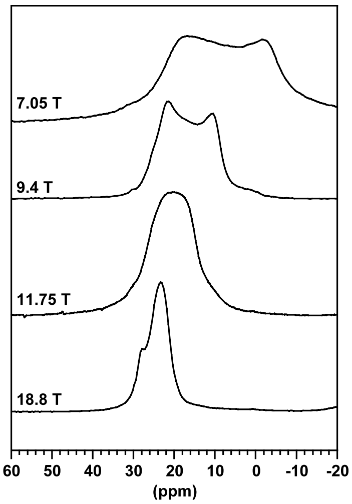

Fig. 6. ^{11}B MAS NMR spectra of Pol(Δ) recorded at various fields.

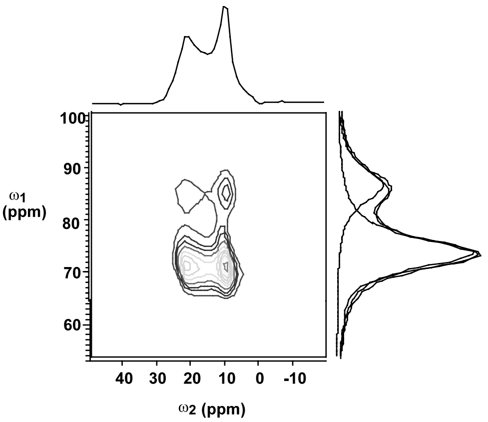

Fig. 7. Two-dimensional ^{11}B MQ-MAS NMR spectrum of Pol(Δ) recorded at 9.4 T with ^{1}H decoupling.

Table 1
List of the various N and B sites identified by ^{15}N and ^{11}B MAS NMR in the three polymers

Polymer	N sites				B sites			
	Proportions (±2%)				Proportions (±2%)			
	N^{III}		N^{IV}		B^{III}		B^{IV}	
Pol(Δ)	$\mathit{N}\mathrm{B}_3$	52	None		$\mathit{B}\mathrm{N}_3$	70	None	
	$\mathit{N}\mathrm{HB}_2$	48			$\mathit{B}\mathrm{HN}_2$	30		
Pol(NH_3)	$\mathit{N}\mathrm{HB}_2$	61	$\mathit{N}\mathrm{H}_2\mathrm{B}_2$	21	$\mathit{B}\mathrm{N}_3$	60	$\mathit{B}\mathrm{H}_2\mathrm{N}_2$	14
			$\mathit{N}\mathrm{H}_3\mathrm{B}$	18	$\mathit{B}\mathrm{HN}_2$	10	$\mathit{B}\mathrm{H}_3\mathrm{N}$	16
PAB	$\mathit{N}\mathrm{HB}_2$	12	$\mathit{N}\mathrm{B}_2\mathrm{H}_2$	68	$\mathit{B}\mathrm{NH}_2$	24	$\mathit{B}\mathrm{H}_2\mathrm{N}_2$	62
			$\mathit{N}\mathrm{H}_3\mathrm{B}$	20			$\mathit{B}\mathrm{H}_3\mathrm{N}$	14

and schematic structural models are proposed in Fig. 8. Pol(Δ), as expected, is mainly based on $[B-N]_3$ rings, even if rings with larger sizes such as $[B-N]_4$ can not be excluded [23]. PAB is based on linear fragments $[BH_2-NH_2]_n$; however, crosslinking reactions have certainly occurred, if one considers the presence of a small number of tricoordinated B and N sites. As for Pol(NH_3), the structure is more complex with certainly a distribution of linear and cyclic fragments; this study strongly suggests that amonolysis of the borazine causes some ring opening reactions, followed by formation of new cyclic structures.

3.2. Pyrolysis products

The three polymers have been heat-treated under inert atmosphere (Ar) up to 1400 °C, where they convert into h-BN with 90, 75 and 65% ceramic yields for Pol(Δ), Pol(NH_3) and PAB, respectively.

The ^{15}N- and ^{11}B-NMR spectra have been recorded on each polymer after heat-treatment to 200 °C (Fig. 9). Interestingly, the B^{IV} and N^{IV} sites present in PAB and Pol(NH_3) have disappeared, and only B^{III} and N^{III} sites remain. Indeed the three polymers have now very similar spectra. The simulations of the ^{15}N CP-MAS spectra reveal the presence of the same set of peaks, with only slight variation in intensity. This suggests that, despite the different architectures of the starting polymeric precursors, a moderate heat treatment to 200 °C, responsible for crosslinking reactions, gives rise to similar polymer networks, based on B^{III} and N^{III} sites. The pyrolysis process of Pol(Δ) has thus been followed.

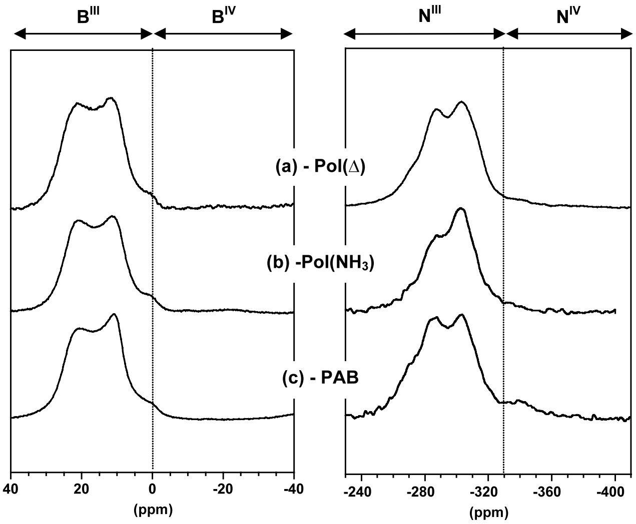

Fig. 9. ^{15}N CP-MAS and ^{11}B MAS NMR spectra of the three polymers heated to 200 °C.

The ^{11}B MAS NMR spectra recorded for the polymer and its pyrolysis products up to 1300 °C (Fig. 10) appear very similar at first sight with a shape characteristic of tricoordinated boron atoms engaged in a B_3N_3 six-membered ring structure [31] ($\delta \approx 30$ ppm, $C_Q \approx 2.8$ MHz, $\eta \approx 0$). As previously described, the use of 2D MQ MAS experiments shows clearly the presence of two types of sites $\mathit{B}\mathrm{N}_3$ and $\mathit{B}\mathrm{HN}_2$ in Pol(Δ) with very close chemical shift values. Another way to distinguish them is to perform a $^1H \rightarrow {}^{11}B$ cross polarization experiment, that will emphasize the protonated site, $\mathit{B}\mathrm{HN}_2$. The Hartmann–Hahn conditions for cross-polarization from $I = 1/2$ (^1H) to $S = 3/2$ (^{11}B) have to be selected properly in order to ensure efficient polarization transfer [32]. The ^{11}B CP-MAS NMR spectra of the starting polymer and the polymer treated at 400 °C are compared in Fig. 11. The simulations show the presence of the expected two sites. The intensity of the directly protonated $\mathit{B}\mathrm{HN}_2$ site is greatly enhanced, especially for short contact times while the intensity of the $\mathit{B}\mathrm{N}_3$ site is comparatively small indicating that this environment is quite far from protons. This suggests the deprotonation

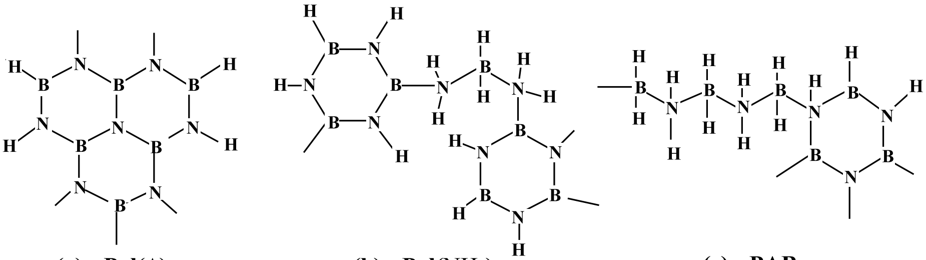

Fig. 8. Schematic representation of the three polymers structures, based on NMR results.

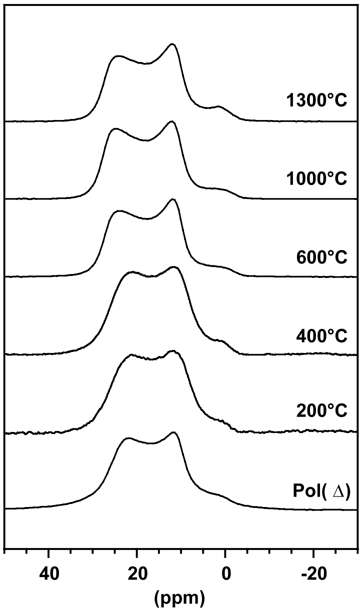

Fig. 10. ^{11}B MAS NMR spectra of Pol(Δ) and its pyrolysis products up to 1300 °C.

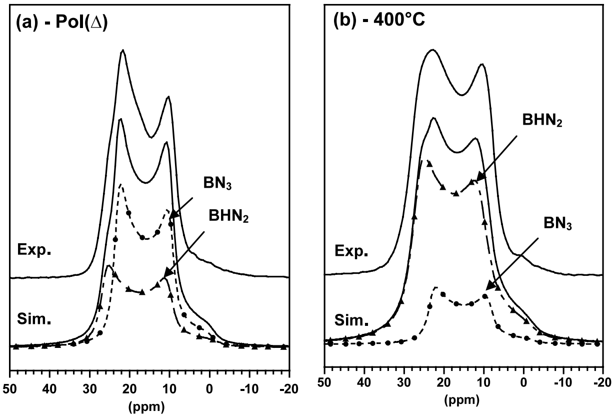

Fig. 11. ^{11}B CP-MAS NMR spectra of Pol(Δ) (a) and Pol(Δ) heat treated at 400 °C (b) (contact time: 160 μs).

of the B sites as confirmed by the comparison of the quantitative ^{11}B MAS spectra of the two samples showing a large decrease of the intensity of the $B\mathrm{HN}_2$ at 400 °C.

The ^{15}N MAS NMR spectra recorded for Pol(Δ) and its pyrolysis products are presented in Fig. 12a. Up to 400 °C, composite signals made of overlapping peaks characteristic of tricoordinated N sites can be seen. The width of the signals and therefore the number of individual components tend to decrease with increasing temperature to give at 800 °C a main signal at −282 ppm. It corresponds to $N\mathrm{B}_3$ sites in h-BN. It is the first time that the ^{15}N signal of h-BN is observed directly. Only a $^{11}\mathrm{B} \rightarrow {}^{15}\mathrm{N}$ CP-MAS spectrum on nonenriched h-BN sample had been reported yet [33]. It also agrees very well with a theoretical calculation that gives $\delta = -285 \pm 5$ ppm [34]. By comparison between SP and CP experiments (Fig. 12b), it appears that signals at high field (≤ -280 ppm) are overestimated by cross polarization, suggesting that they correspond to protonated sites. As mentioned previously, ab initio calculations of ^{15}N-NMR chemical shifts have been performed on model clusters to help in the identification of the various ^{15}N sites [29]. Six N environments have been considered (Fig. 4), that can be divided in two types if one considers only the first coordination sphere, $N\mathrm{B}_3$ (▲, ◆, ★) and $N\mathrm{HB}_2$ (●, ▼, ■). The corresponding chemical shift values have been reported in Fig. 12. A good agreement is observed between the calculated peak positions and the spectral changes during pyrolysis. A mild heat treatment to 200 °C causes a disappearance of the peaks at low field (> -270 ppm), which are indeed assigned to $N\mathrm{B}_3$ (▲) and $N\mathrm{HB}_2$ (●) sites with two B–H bonds. Up to 400 °C, no large changes are observed, while at 800 °C, one signal is now dominant, which is assigned to $N\mathrm{B}_3$ sites in h-BN (★). However, the CP spectrum reveals at this temperature the presence of residual protonated sites: the signal at −305 ppm is indeed assigned to $N\mathrm{HB}_2$ sites with no B–H bonds (■). At 1450 °C, a unique signal is observed, assigned to h-BN as suggested by the X-ray diffraction data. The evolution of these spectra suggests that the ceramization process occur through a preferential disappearance of B–H bonds. A summary of the N sites identified at different temperatures are listed in Table 2.

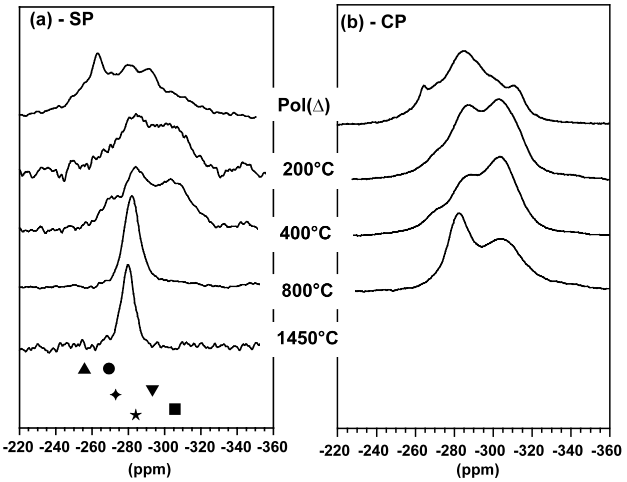

Fig. 12. ^{15}N SP-MAS (a) and CP-MAS (b) spectra of Pol(Δ) and its pyrolysis products up to 1450 °C. Symbols added in (a) refer to the position of the different nitrogen environments decribed in Fig. 4.

4. Conclusion

The objective of this paper was to illustrate the range of structural information that can be obtained through the use of solid state NMR, on boron nitride preceramic

Table 2
List of the various N sites identified by ^{15}N MAS NMR in Pol(Δ) heat-treated at 200, 400, 800 and 1450 °C

Assignment	Proportions (±2%)				
	200 °C	400 °C	800 °C	1500 °C	
NB_3	▲	9	7	–	–
NB_2H	●	–	–	–	–
NB_3	◆	15	18	9	–
NB_3	★	15	22	77	100
NB_2H	▼	27	18	–	–
NB_2H	■	15	19	14	–

Symbols refer to the position of the different nitrogen environments described on Fig. 4.

polymers and their pyrolysis products. Different techniques are now available to improve resolution and spectral edition for ^{15}N and ^{11}B spectra, and thus to get a good description of the local order around N and B sites. However, the lack of sensitivity of ^{15}N makes the preparation of enriched samples necessary; otherwise, only $^{1}H \rightarrow ^{15}N$ CP experiments can be performed, which restrain the study to protonated samples, and prevents any quantitative analysis.

Three BN preceramic polymers have been studied, two polyborazilenes prepared from borazine, either through thermolysis (Pol(Δ)) or amonolysis (Pol(NH_3)) and a poly(aminoborane) $[NH_2BH_2]_n$ (PAB). With single pulse experiments, it was easy to distinguish tetra- and tricoordinated sites, due to the large chemical shift range: only tricoordinated B^{III} and N^{III} sites were found in Pol(Δ), mainly tetraccordinated B^{IV} and N^{IV} sites in PAB and a mixture of tri- and tetracoordinated sites in Pol(NH_3). Then a sequence, called IRCP derived from CP was successfully applied to differentiate, within each family (N^{III} and N^{IV}), the various ^{15}N overlapping signals. In Pol(Δ), seven signals were identified, corresponding to two types of environment, $\mathit{N}B_3$ and $\mathit{N}HB_2$. The multiplicity of the resonance signals demonstrates the high sensitivity of the ^{15}N chemical value, not only to the first neighboring atoms, but also to the second ones, in perfect agreement with published ab initio calculations. The ^{11}B chemical shift values are much less sensitive to differences in first neighboring atoms and the quadrupolar nature of this isotope may cause strong broadening of the lines. For Pol(Δ) and Pol(NH_3), 1D MAS spectra recorded at 18.8 T allowed a good separation of signals when the chemical shift difference was higher than 5 ppm. However, in Pol(Δ), 2D MQ-MAS sequence coupled with strong ^{1}H decoupling was the most efficient technique to reveal the presence of the two expected B sites, $\mathit{B}N_3$ and $\mathit{B}HN_2$. This was also confirmed by $^{1}H-^{11}B$ CP-MAS experiments. A combination of all these NMR techniques allowed us to identify and even quantify, even if not with high accuracy, the various B and N sites present in the three BN polymers. The first neighboring atoms were identified, and even the second ones for ^{15}N, which allowed us to propose some schematic structural models for the three polymers.

Then the polymer-to-ceramics transformation was followed through the study of samples pyrolyzed at selected temperatures, from 200 to 1450 °C. Interestingly, despite the differences in their initial architecture, the structures of the three polymers are very similar after crosslinking at 200 °C, with the presence of only tricoordinated sites. $^{1}H-^{15}N$ and $^{1}H-^{11}B$ CP experiments were used to follow the consumption of N–H and B–H bonds. Due to the large sensitivity of the ^{15}N chemical shift values to the first and second neighboring atoms, the series of ^{15}N MAS NMR spectra recorded on the pyrolyzed products, allowed us to get a good picture of the change in N environments. By 800 °C, the ^{15}N SP-MAS NMR spectra shows one main resonance signal due to h-BN, suggesting that the ceramization step is almost finished at this relatively low temperature.

Acknowledgements

The authors would like first to greatly acknowledge the synthetic chemists who prepared all the preceramic polymers, including some ^{15}N enriched ones: E.F., C.D. and M.V. from University of Rennes (France) and D.-P.K. from Chungnam University (Korea). Then they would like to thank the persons who gave them the possibility to run all the NMR spectra that are presented in this paper: J.M. (CMC, Paris, France), P.F. and D.M. (CRMHT-CNRS, Orléans, France), P.T. and J.B.d'E. (ESPCI, Paris, France) and S.S. (Bruker, Karlsruhe, Germany).

References

[1] J. Bill, F. Aldinger, Adv. Mater. 7 (1995) 775.
[2] M. Birot, J.-P. Pillot, J. Dunogues, Chem. Rev. 95 (1995) 1443.
[3] R.M. Laine, F. Babonneau, Chem. Mater. 5 (1993) 260.
[4] R.T. Paine, C.K. Narula, Chem. Rev. 90 (1990) 73.
[5] D. Seyferth, W.S. Rees, Jr., Chem. Mater. 3 (1991) 1106.
[6] P.J Fazen, J.S Beck, A.T. Lynch, E.E. Remsen, L.G. Sneddon, Chem. Mater. 2 (1990) 96.
[7] K.-T. Moon, D.-S. Min, D.-P. Kim, Bull. Korean Chem. Soc. 19 (1998) 222.
[8] F. Guilhon, B. Bonnetot, D. Cornu, H. Mongeot, Polyhedron 15 (1996) 851.
[9] F. Thévenot, C. Doche, H. Mongeot, F. Guilhon, P. Miele, D. Cornu, B. Bonnetot, J. Solid State Chem. 133 (1997) 164.
[10] D. Cornu, P. Miele, R. Faure, B. Bonnetot, H. Mongeot, J. Bouix, J. Mater. Chem. 9 (1999) 757.
[11] O. Funayama, T. Kato, Y. Tashiro, T. Isoda, J. Am. Ceram. Soc. 76 (1993) 717.
[12] R. Riedel, J. Bill, A. Kienzle, Appl. Organomet. Chem. 10 (1996) 241.

[13] H.-P. Baldus, M. Jansen, Angew. Chem. Int. Ed. Engl. 36 (1997) 328.

[14] T. Wideman, P.J. Fazen, K. Su, E.E. Remsen, G.A. Zank, L.G. Sneddon, Appl. Organomet. Chem. 12 (1998) 681.

[15] M. Weinmann, R. Haug, J. Bill, M. de Guire, F. Aldinger, Appl. Organomet. Chem. 12 (1998) 725.

[16] M. Weinmann, J. Scuhmacher, H. Kummer, S. Prinz, J. Peng, H.-J. Seifert, M. Christ, K. Müller, J. Bill, F. Aldinger, Chem. Mater. 12 (2000) 623.

[17] B. Jaschke, U. Klingebiel, R. Riedel, N. Doslik, R. Gadow, Appl. Organomet. Chem. 14 (2000) 671.

[18] R. Riedel, A. Kienzle, W. Dressler, L. Ruwitsch, J. Bill, F. Aldinger, Nature 382 (1996) 796.

[19] F. Babonneau, J. Maquet, C. Bonhomme, R. Richter, G. Roewer, D. Bahloul, Chem. Mater. 8 (1996) 1415.

[20] T. Wideman, L.G. Sneddon, Inorg. Chem. 34 (1995) 1002.

[21] E. Framery, PhD dissertation, University of Rennes, France, 1996.

[22] D.-P. Kim, K.-T. Moon, J.-G. Kho, J. Economy, C. Gervais, F. Babonneau, Polym. Adv. Technol. 10 (1999) 702.

[23] C. Gervais, J. Maquet, F. Babonneau, C. Duriez, E. Framery, M. Vaultier, P. Florian, D. Massiot, Chem. Mater. 13 (2001) 1700.

[24] D. Massiot, F. Fayon, M. Capron, I. King, S. Le Calv, B. Alonso, J. Durand, B. Bujoli, Z. Gan, G. Hoatson, Magn. Reson. Chem. 40 (2002) 70.

[25] E. Framery, M. Vaultier, Heteroat. Chem. 11 (2000) 218.

[26] X. Wu, K.W. Zilm, J. Magn. Reson. Sect. A 102 (1993) 205.

[27] R. Sangill, N. Rastrup-Andersen, H. Bildsoe, H.J. Jakobsen, N.C. Nielsen, J. Magn. Reson. 107 (1994) 67.

[28] C. Gervais, F. Babonneau, J. Maquet, C. Bonhomme, D. Massiot, E. Framery, M. Vaultier, Magn. Reson. Chem. 36 (1998) 407.

[29] M. Gastreich, C.M. Marian, J. Comput. Chem. 19 (1998) 716.

[30] A. Medek, J.S. Harwood, L. Frydman, J. Am. Chem. Soc. 117 (1995) 12779.

[31] P.S. Marchetti, D. Kwon, W.R. Schmidt, L.V Interrante, G.E. Maciel, Chem. Mater. 3 (1991) 482.

[32] A.J. Vega, Solid State NMR 1 (1992) 17.

[33] G. Jeschke, W. Hoffbauer, M. Jansen, Solid State NMR 12 (1998) 1.

[34] C.M. Marian, M. Gastreich, Solid State NMR 19 (2001) 29.